INDIAN JOURNAL OF SCIENCE AND TECHNOLOGY

RESEARCH ARTICLE

Computational Investigation of Under Expanded Solar Chimney Power Plant

C K Akhil[1], Rajamurugu Natarajan[2]*, S Yaknesh[2]

1 Research Scholar, Department of Aeronautical Engineering, Bharath Institute of Higher Education and Research, Chennai, India
2 Assistant Professor, Department of Aeronautical Engineering, Bharath Institute of Higher Education and Research, Chennai, India

OPEN ACCESS

Received: 10-02-2023

Accepted: 03-07-2023

Published: 24-08-2023

Citation: Akhil CK, Natarajan R, Yaknesh S (2023) Computational Investigation of Under Expanded Solar Chimney Power Plant. Indian Journal of Science and Technology 16(32): 2485-2493. https://doi.org/10.17485/IJST/v16i32.293

* **Corresponding author**.

rmnshivsai1210@gmail.com

Funding: None

Competing Interests: None

Published By Indian Society for Education and Environment (iSee)

ISSN
Print: 0974-6846
Electronic: 0974-5645

Abstract

Objectives: To study the effect of the Area Ratio of the chimney and collector on the driving potential of a Solar Chimney Power Plant (SCPP) using computational studies. **Methods:** The chimney whose area ratio (AR) is greater than unity is tested for three different collector shapes. The under-expanded chimneys are subjected to different collector configurations namely fully slopped, and sloped at midway. The computational analyses are carried out in ANSYS-FLUENT R2021. The temperature, velocity, and static pressure are compared with the Manzarnes prototype properties and found that the fully sloped collector is behaving best in comparison with the other two configurations. Then, a vertical Convergent Divergent (C-D) chimney with a fully sloped collector was investigated in at open environment in real-time conditions. Thermocouple, Anemometer is used to measure the temperature and anemometer respectively. **Findings:** The average temperature rise inside the SCPP is found to be 10K in the simulation studies using ANSYS-FLUENT. Sloped at midway collector configuration (case-2) achieved a peak velocity of 1.4m/s which is 12% superior to the fully slopped configuration (case-1). The case-1 outperformed the manzarnes plant by 23%. The Convergent Divergent (C-D) chimney with a fully sloped collector (case-3) behaves poorly which is inferior by 23%, and 12% to case-1 and case-2 respectively. **Novelty:** The novelty of this work lies in the comparison and simulation of three different configurations of the SCPP. This study is useful to society as it provides valuable insights into the design and optimization of solar power plants. The findings of this study can be used by engineers and energy experts to improve the efficiency of solar power plants, reduce the cost of energy production, and contribute to the global effort toward sustainable energy sources. The study also highlights the importance of considering different configurations and design elements in the optimization of solar power plants.

Keywords: Solar chimney; CFD; Area Ratio; Experimentation; AeroThermal dynamics

1 Introduction

Solar Chimney Power Plants (SCPPs) have gained recognition as promising solution for generating green energy. SCPPs not only provide a sustainable means of producing electricity but also offer potential applications in natural ventilation, crop drying in arid regions, and desalination of seawater. The fundamental principle behind a solar chimney involves the upward movement of air driven by the density difference under a transparent collector and the pressure variation in the chimney from the base to the vent. Turbines, placed inside the chimney or at the collector-chimney junction, harness the kinetic energy of the updraft to generate electricity. Significant research has been conducted on SCPPs, with a particular focus on investigating the impact of geometric parameters on system performance.

In recent years, researchers have increasingly explored the relationship between system efficiency and geometric parameters through simulation and experimental studies. However, several research gaps still exist in this domain(1). Previous numerical studies have examined the influence of collector inclination on chimney efficiency and observed significant changes in flow parameters such as velocity, pressure, and temperature. However, there is a need for further investigation to comprehensively understand the effects of collector inclination on system performance(2).

Furthermore, studies have sought to optimize SCPPs based on regional climatic data and geometric parameters. Researchers have found that increasing collector and chimney radii lead to higher air outflow velocities, while taller collectors harm system performance. However, more extensive research is required to determine the optimal geometric configurations for maximizing power output(1,3).

The divergent angle of the chimney is another crucial parameter that influences power generation. Computational studies have shown that increasing the chimney's divergent angle reduces the rate of power generation improvement. Additionally, the solar radiation and chimney radius directly affect power generation, with an optimal divergent angle resulting in maximum power output(4). However, further investigation is needed to determine the ideal divergent angle and its impact on system performance.

The influence of the collector inclination angle has also been explored. Studies have demonstrated that a collector tilt angle of 35 degrees enhances the collector's absorption capacity(5). Moreover, inclined collectors and thermal energy storage devices have been shown to significantly increase collector power production per unit area. A study(6) explores the methods to improve thermo-aerodynamic parameters in chimney solar power plants using mini hemispherical concentrators. Compared to conventional designs, the prototype shows a 24.4% improvement in thermal field, 58.6% in dynamic field, and achieves a thermal efficiency of 68.88%, the prototype achieved velocity of 2.87m/s. However, more research is needed to investigate the impact of collector inclination angle on thermal efficiency, collector efficiency, and power production(7,8).

Another research gap relates to the influence of chimney shape on SCPP performance. Comparative studies have shown that divergent chimneys outperform cylindrical chimneys, with a 54% improvement in performance(9). A study(10) examines the impact of chimney inclination (15°, 22°, and 30°) on the performance of freestanding updraft chimney solar power plants. It considers a straight rigid tower and a tilting tower under wind forces. Results indicate that a tower inclination of up to 22° enhances SCPP performance and improves energy utilization with reduced entropy generation. Additionally, the chimney's divergence angle has been found to affect power output, with a divergence angle of 2 degrees yielding optimal results(11). However, further investigation is required to determine the optimal chimney shape and divergence angle for enhanced performance.

Additionally, the effect of thermal energy storage systems on SCPP performance, particularly after sunset when solar radiation is unavailable, requires further exploration. Studies have shown that SCPPs equipped with thermal energy storage outperform those without storage under such conditions(12). A recent study(13) uses numerical simulation to analyze turbulent fluid flow in a solar chimney power plant (SCPP). Geometric modifications are made at the chimney outlet with soil as the storage system below the collector and another with 10 cm thick water-filled tub covering the collector surface. This study analysed the impact of storage systems on plant performance and operation duration after sunset. It is also proven in a recent research(14) that the thermal storage system enhances the maximum speed of the flow which is absent in other systems which didn't utilised any ground storage systems.

Lastly, there is a lack of comprehensive research on the practical implementation and performance evaluation of medium-scale SCPPs. While some studies have described the process of building medium-scale SCPPs and their electricity generation, there is a need for further investigations and comprehensive datasets to validate mathematical models proposed by researchers(14).

In light of these research gaps, this study aims to contribute to the field of SCPPs by conducting both experimental and computational studies on various collector and chimney configurations. The simulation results will be presented alongside experimental data to provide a comprehensive analysis. By addressing the aforementioned research gaps, this study aims to enhance our understanding of SCPPs and their potential as sustainable energy solutions.

2 Methodology

The proposed approach in this study introduces novel aspects of solar chimney power plants (SCPPs). It incorporates a divergent chimney model, increasing efficiency by considering the energy transformation from solar absorption to airflow kinetic energy. Different collector configurations are explored, optimizing chimney diameter, collector diameter, and tilt.

In a basic form, the fundamental equation linking to the efficiency of all system components is given where the solar tower's power output P is represented as

$$Power\ Output\ (P) = q_{solar}\ \ \eta_{coll}\ \ \eta_{tur}\ \ \eta_{tower} \tag{i}$$

Where,

Qsolar - Input Solar Energy

η_{coll} - Collector Efficiency

η_{tur} - Turbine Efficiency

η_{tower} -Tower Efficiency

The maximum velocity equation can be simplified further by boussinesq approximation.

$$V_{max} = \sqrt{2gH\frac{(\Delta T)}{T_o}} \tag{ii}$$

The efficiency of the tower equation simplifies to,

$$\eta_{tower} = \frac{gH}{C_p\ T_o} \tag{iii}$$

The updraft velocity represented by Equation (iii) is located near the bottom of the plant, in that place it achieves the highest or peak velocity, so it is recommended to place the wind turbine at that position. The produced upward directional velocity is influenced by gravity, the temperature of the airflow, ambiance temperature, and solar tower height. The updraft velocity equation (ii) is meant to convert the upthrust velocity of the air to the mass flow rate by altering the ratio of the collector area to the area of the tower.

$$m = \rho A_{coll}\ V = \rho\pi r^2 = \rho\pi r^2\sqrt{2gH\frac{(\Delta T)}{T_o}} \tag{iv}$$

The Temperature of the airflow is used to determine density. By increasing the radius of the chimney presents another building issue. As a result, an optimised chimney diameter, collector diameter, and collector tilt must be thoroughly investigated. A Divergent chimney, As illustrated inFigure 1, the tower efficiency equation is updated by taking into account the inflow to the collector at speed V_2 and exiting the diverging chimney with velocity V_3. The assumption made are earth surface has uniform heat collection and steady-state temperature within the collector.

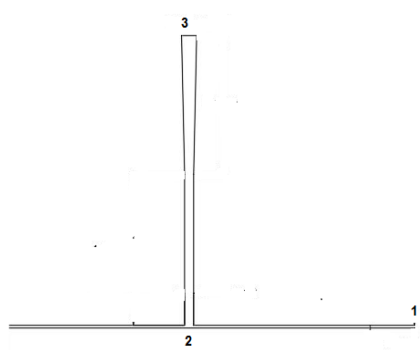

Fig 1. Chimney – Divergent Model

The velocity of the fluid flow departing the base of the chimney due to the temperature rise can be expressed as,

$$v_2 = \sqrt{2gh\frac{\Delta T}{T}} \tag{v}$$

Power induced by fluid flow is,

$$\frac{1}{2}\dot{m}V_{\max}^{2} = \frac{q'' A_r \beta}{C_p} gh_c \tag{vi}$$

The Efficiency of the system by definition,

$$\eta_{\text{tower}} = \frac{\beta gHc}{Cp} \tag{vii}$$

we know that β= 1/T for a perfect gas, the solar tower efficiency is influenced by various parameters some affect directly some indirectly in this scenario the chimney height is directly proportional and inversely proportional to the intake temperature of the collector, but temperature rise in the collector is an independent parameter.

The change is pressure or the driving potential which is represented as 'P' is the reason for the airflow from the intake of the collector to the top of the chimney which is the pressure difference created between atmospheric or ambient pressure at the ground and the airstream static pressure at the base of the chimney which can be expressed as follows,

$$\Delta p = (\rho_o - \rho)\, gH_{chi\ m} + 0.5\rho V_2^2 \left[1 - \frac{A_3^2}{A_2^2}\right] \tag{viii}$$

When $A_3 = A_2$, the above equation corresponds to a straight cylindrical chimney or a correctly expanded chimney. Power production is proportional to the loss in pressure between the turbine and the rate of flow of the air stream. In this investigation a 2D model is considered which doesn't implement a turbine rather a pressure drop of the turbine is considered and power is estimated for the SCPPs, i.e.,

$$P_{out} = x \triangle P_{tot} V_t A_{coll} \tag{ix}$$

P_{tot} signifies the system's total driving potential, while factor x is the ratio of the drop in pressure over the turbine to the system's total driving potential. The greatest potential pressure decrease under the premise of a constant-driving-potential system is x = 2/3[12].

The theoretical model developed in this study for divergent solar chimneys extracts that the energy transformation from solar energy absorbed in the chimney to the kinetic energy of the airflow at the base of the chimney is increased by a factor of $(A_3/A_2)^2$, here A_2 is the area of the chimney base and A_3 is the cross-sectional area of the chimney top.

The efficiency of the solar chimney with a divergent shape is doubled by $(A_3/A_2)^2$. In the present study, the under expanded chimneys are subjected to different collector configurations namely fully slopped collector(case-1), sloped midway collector(case-2) and vertical Convergent Divergent chimney with fully sloped collector (case-3) as shown in Figure 2. The flow properties inside the chimneys are analysed using computational and experimental techniques.

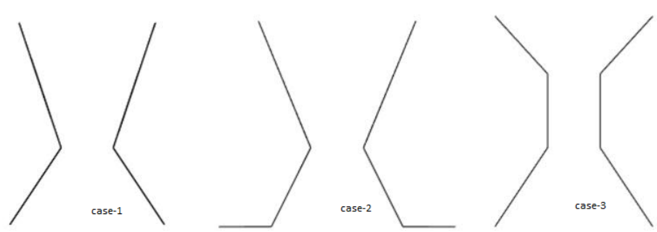

Fig 2. Solar Chimney structures considered for the study

2.1 Computational Studies

Ansys-Fluent R2021 is used in this work to examine the flow characteristics within the SCPP by solving the Navier-Stokes Equations. In the constructed models of the solar chimney power plant, the K-epsilon model is used to observe turbulence. A few flow assumptions are established, and they are as follows;

1. Steady fluid flow

2. Three-Dimensional flow and flow are turbulent.
3. Axisymmetric flow field.
4. Fluid is binding with Boussinesq Approximation.

The simulation is then completed by appropriate model mesh. Initial clean up is carried out to the meshed model in fluent software as the initial step of pre-processing after importing the model. The imported model is then set up to give proper boundary conditions. The gravity on the negative Z-axis is specified as 9.81 m/s^2 in the typical arrangement. Discrete Ordinates (DO) system is used to represent radiation inside the solar chimney. The boundary conditions given in the simulation model allow the solid zone to contribute in radiation as a transparent medium. Solar tracking is utilised in this model to trail the radiation intensity on the length and breadth of the chimney area installed.

To define the flow property of natural convection and intensity, the buoyance Rayleigh number (Ra) is a proper choice. If the Ra number is greater than 10^9 the flow reaches turbulence inside the solar chimney, k-epsilon two-equation viscous model is implemented, and for analysing the turbulent condition RNG model is used.

The simulation's governing equations [13];

Continuity equation:

$$\frac{\partial(\rho u)}{\partial t} + \nabla \bullet \rho \overrightarrow{V} = 0 \tag{1}$$

Momentum equation:

$$\rho\left[\frac{\partial \overrightarrow{v}}{\partial t} + \overrightarrow{V} \bullet \nabla \overrightarrow{V}\right] = -\nabla p + \mu \nabla^2 \overrightarrow{V} + \frac{1}{3}\mu\nabla\left(\nabla \bullet \overrightarrow{V}\right) + \overrightarrow{F_b} \tag{2}$$

Energy equation:

$$\frac{\partial(\rho e_t)}{\partial t} + \nabla \bullet \left[\overrightarrow{V}(\rho e_t + p)\right] = \nabla \bullet \left[k \nabla T + \left(\overset{\tau}{\bullet}\overrightarrow{V}\right)\right] + \dot{S_g} \tag{3}$$

k-ε equations:

$$\frac{\partial}{\partial t}(\rho k) + \frac{\partial}{\partial x_j}(\rho k u_j) = \frac{\partial}{\partial x_j}\left[\left(\mu + \frac{u_t}{\sigma_k}\right)\frac{\partial k}{\partial x_j}\right] + G_k + G_b - \rho\varepsilon - Y_M + S_k \tag{4}$$

and

$$\frac{\partial}{\partial t}(\rho\varepsilon) + \frac{\partial}{\partial x_j}(\rho\varepsilon u_j) = \frac{\partial}{\partial x_j}\left[\left(\mu + \frac{\mu_t}{\sigma_\varepsilon}\right)\frac{\partial \varepsilon}{\partial x_j}\right] + \rho C_1 S\varepsilon - \rho C_2 \frac{\varepsilon^2}{k + \sqrt{v\varepsilon}} + C_{1\varepsilon}\frac{\varepsilon}{k}C_{3\varepsilon}G_b + S_\varepsilon \tag{5}$$

where,

$C_1 = max\left[0.43, \frac{\eta}{\eta+5}\right], \eta = S\frac{k}{\varepsilon}, S = \sqrt{2S_{ij}S_{ij}}$.

2.2 Boussinesq Approximation

The SCPP simulates the buoyancy effect. By approximating the air density is held constant in governing equation,

$$(\rho - \rho 0)g = -\rho 0 \beta (T - T_0) g \tag{6}$$

here, T_0 = Buoyancy Temperature (Reference)

g = Gravity (9.81 m/s2)

β = fluid rate of expansion.

ρ_0 = Density at ambient conditions.

Power output:

$$P_{out} = \dot{m} g H_c \frac{\triangle T}{T_a} \tag{7}$$

Where $\dot{m} = \rho AV$ = flow rate

2.3 Boundary Conditions (BC's)

BCs based on actual flow conditions were included to analyse the domain's flow physics. The cell zone conditions for operation are reported as 303K and 1 atm pressure. The following highlights the materials' thermo-physical characteristics that were chosen for the numerical study.

i) Boundary conditions for the pressure at the inlet and outlet were given at the collector entrance and chimney exit respectively.

ii) The working fluid's subsequent thermo physical characteristics were used: Thermal conductivity (k) = 0.0242 W/ mK, thermal diffusivity (d) = 2.137 105 m2/s, specific heat (Cp) = 1006 J/kgK, and density (ρ) = 1.125 kg/m3.

iii) Partially transparent collector cover material is implemented.

iv) The heat transfer coefficient (h) for convection BC was 8 W/m^2 K.

v) Where (ρ = 2702 kg/m3, k = 0.78 W/mK, Cp= 840 J/kgK, absorption coefficient (a)= 0.3 m-1, transmittance and refractive index are 0.9 and 1.562, respectively, high transmittance glass was chosen as the collector cover material

vi) Modeling the chimney wall using the adiabatic wall condition

vii) Chimney material is galvanised iron, collector material is plastic film and ground material is sand.

2.4 Solution Methods

i) The solution approach for pressure-volume coupling is a straightforward strategy. For pressure PRESTO, momentum, turbulent kinetic energy, turbulence dissipation rate, and energy second-order upwind, the solution techniques employed.

ii) First-order upwind is employed for Discrete Ordinates. The solution is initiated and iterated with the convergence criteria set to 10^{-6}. The produced models are loaded into ANSYS ICEM - CFD for meshing.

iii) Tetrahedral element is used to discretise the model domain.

iv) Table 1 provides number of nodes and elements used in each model specified.

v) The mesh used for all four models are the tetrahedral structure, working fluid is air.

Table 1. Meshing Particulars

	Case 1	Case 2	Case 3	Case 4
Nodes	51978	69479	26855	56041
Elements	269567	369887	122351	292993

2.5 Grid Independence Study

Grid adaptation based on flow velocity gradients was used to assess if the computed that solution generated for flow is not dependent of the meshed elements. Because the solar chimney flow provides a level result, the curvature technique was utilised, Since the residual values are not normalised standard normalization is implemented. In addition, a 25% refine threshold is set.

In the simulation process initially Manzanares solar tower was taken for calibration and the answers are validated, Then the simulation for our current investigation is carried out.

3 Results and Discussion

The collected results are anticipated to yield information that will help improve the SCPP's overall effectiveness. The following paragraphs describe the flow process in cases- 1& 2 with simulation and experimental results.

In the axially symmetric plane of the SCPP, for case-1, the distribution of the velocity intensity is depicted in Figure 3. These findings show that peak values have been seen close to the chimney's inlet. The air velocity value decreases from bottom to top along the chimney axis. This is because the driving potential is maximum at the chimney inlet. Before monitoring the value of the air velocity outside the prototype, magnitude velocity measurements along the collector begin to decline dramatically away from the chimney axis.

Figure 4 (a) and (b) validate these findings by showing the air velocity profiles along the collector radius and chimney axis in that order. By concentrating on these results, a variation in the maximum value of the magnitude velocity between cases is noted. It has been observed when examining the two cases (Cases 1&2) that an increase in collector diameter leads to a rise in magnitude velocity.

The distribution of the static pressure for both cases is depicted in Figure 5 in the axisymmetric plane of the SCPP. These findings show that a slump zone, present in all chimney layouts, is situated at the chimney's base. However, it is noted that

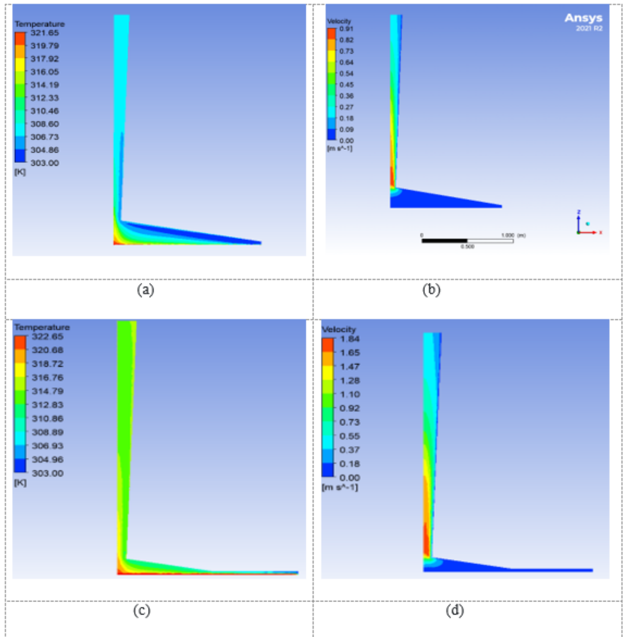

Fig 3. (a) Temperature contour of case-1 (b) Velocity contour of case-1 (c) Temperature contour of case-2 (d) Velocity contour of case-2

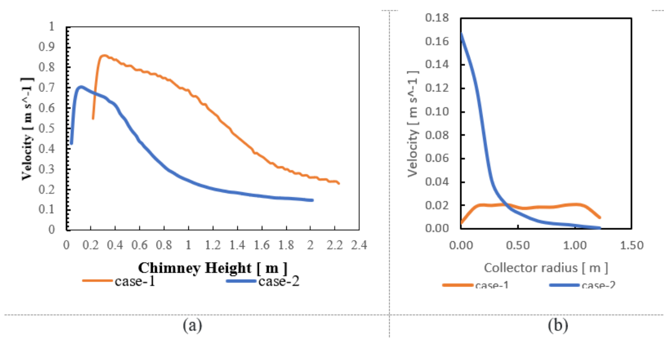

Fig 4. (a) Variation of velocity along chimney (b) Variation of velocity along collector

there is a compression zone in the collector and at the top of the chimney. The slump zone observed around the chimney's base is where the differences between the cases under consideration are primarily visible. The slump zone's inhabited area is distinct from Figure 3 (a) and (b). The gradient between the collector output and inlet then becomes rather large. It has been noted that in all circumstances, the temperature under the collector rises by roughly 10 K. This is a result of the air under the collector having a low volume. The values of the air temperature fall as they move out from the centre until they reach the outlet's ambient temperature (from Figure 3 c & d). Because the collector efficiency is directly related to the temperature differential in the system, this fact may help to increase it. Due to the adiabatic designed chimney and the low height, the airflow in the chimney zone continues to be increasing.

The present numerical results of case-1 are compared with the simulation data from the work [9] by plotting the dimensionless velocity (v/V_{max}) against the dimensionless chimney radius (r/Ro) presented in Figure 5. The comparison was done at a section across the chimney bottom just above the transition region. The results showed a good agreement between the present numerical results and the data from [9].

The velocity contour of the case-3 shown in Figure 6 (a) has given the following observations. The horizontal movement of air stream inside the vertical chimney is considerably higher at the inlet rather than any section. As it approaches the vertical chimney due to expansion of the chimney at the top as well as in the bottom the velocity decreases at the chimney inlet however

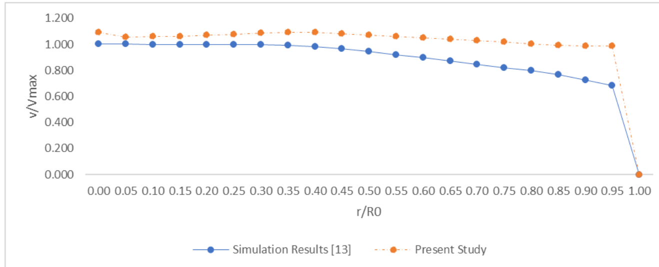

Fig 5. Validation of case 1 with existing study

the air stream gains momentum and picks up the energy due to enlargement of the air passage. The velocity reaches its peak value of 0.6m/s, but found to be least among other cases considered in this research.

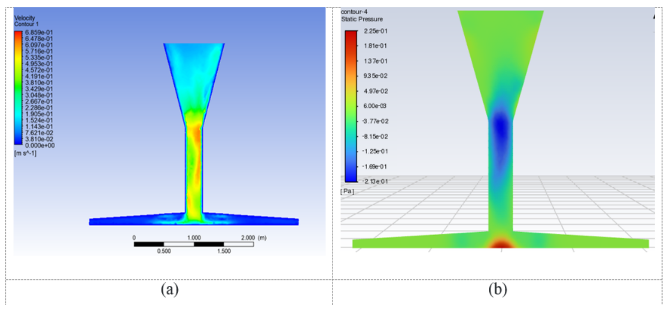

Fig 6. (a) Velcoity contour of case-3 (b) Temperature contour of case-3

The pressure inside the chimney raises near the inlet due to the flow disturbances hence the magnitude is minimum. Later, the pressure increases because of the expansion of the chimney at the top where relatively the velocity decreases. The experiment on a prototype plant of height 2m with collector radius of 1.5m is also validated with the computational studies shown in Figure 7 below. In the experimental study of case-3 the maximum velocity was obtained near the chimney wall, and that the velocity increased with height. Additionally, the velocity profile was plotted for the location of the turbine blade section and the maximum velocity was found to be near the wall. The simulation results of case-3 are compared with the experimental work[11] by plotting the dimensionless velocity (v/V_{max}) against the dimensionless chimney radius (r/Ro) in Figure 7.

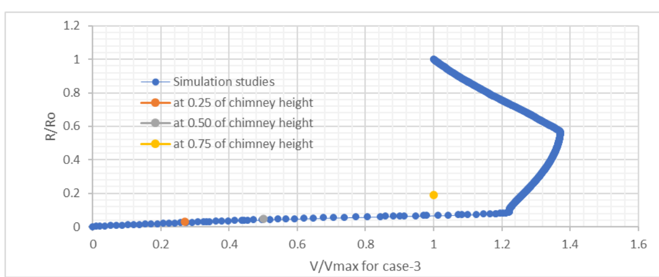

Fig 7. Comparison of simulation results with existing study[11]

The comparison is found to be similar with the experimental results. The Figure 8 shows the variation of air velocity at different (r/Ro) of a chimney. It was observed that the average velocity of air at the chimney base reaches a maximum and gradually decreases towards the outlet. The experimental results are seeming to be in close agreement with the study[15].

Of the all-divergent chimneys considered in the present study the effect of area ratio is clearly witnessed by the velocity magnitude at the base of the chimney. The case-1 peak magnitude velocity is 1.6m/s which is 50% higher than the manzarnes plant. The temperature rise is found to be 10K in the simulation studies. Case-2 achieved a peak velocity of 1.4m/s which is 12% inferior to the case-1 but still out performed the manzarnes plant by 23%. The case-3 behaves poorly due to the heat at the top

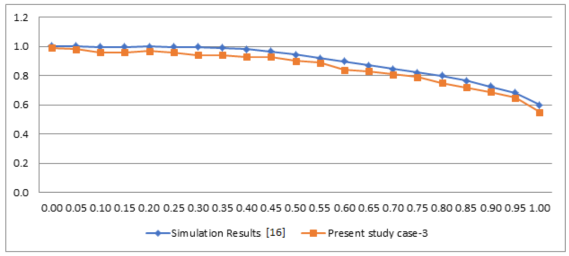

Fig 8. Validation of case-3 simulation results with existing study [15]

hence it is lowered by 23% compared to case-1 and by 12% in case-2.

4 Conclusion

To reduce investment costs and boost power output, the solar chimney power plant needs to be optimised. This report illustrates the impact of the solar chimney power plant's area ratio such as the diverging chimneys with sloped collector. In fact, the presentation and discussion of the effect of the chimney expansion on the regional airflow characteristics. For each scenario, the magnitude velocity, temperature, static pressure, and power output were shown. Results comparing the various systems demonstrate that the totally divergent chimney boosts power. Case 1 has 50% higher velocity magnitude and 10K temperature rise compared to the Manzarnes plant. Case 2 has 12% lower velocity magnitude but still outperforms the Manzarnes plant by 23%. Case 3 has 23% lower velocity magnitude and performs poorly due to high temperature. For designers of new or current solar chimney power plants, these results are helpful.

References

1) Mehranfar S, Gharehghani A, Azizi A, Andwari AM, Pesyridis A, Jouhara H. Comparative assessment of innovative methods to improve solar chimney power plant efficiency. *Sustainable Energy Technologies and Assessments*. 2022;49:101807. Available from: https://doi.org/10.1016/j.seta.2021.101807.
2) Ayadi A, Driss Z, Bouabidi A, Abid MS. Effect of the number of turbine blades on the air flow within a solar chimney power plant. *Proceedings of the Institution of Mechanical Engineers, Part A: Journal of Power and Energy*. 2018;232(4):425–436. Available from: https://doi.org/10.1177/0957650917733128.
3) Hooi LB, Thangavelu SK. A parametric simulation of solar chimney power plant. *IOP Conference Series: Materials Science and Engineering*. 2018;297:012057. Available from: https://doi.org/10.1088/1757-899x/297/1/012057.
4) Ridwan A, Hafizh H, Fauzi MR. Design and experimental test for solar chimney power plant: case study in Riau Province, Indonesia. *IOP Conference Series: Materials Science and Engineering*. 2018;403:012092. Available from: https://doi.org/10.1088/1757-899x/403/1/012092.
5) Das P, Chandramohan VP. Estimation of flow parameters and power potential of solar vortex engine (SVE) by varying its geometrical configurations: A numerical study. *Energy Conversion and Management*. 2020;223:113272. Available from: https://doi.org/10.1016/j.enconman.2020.113272.
6) Ouédraogo S, Ousmane M, Mogmenga L, Ky TSM, Kam S, Bathiébo JS. Experimental Study of the Airflow in Natural Convection in an Innovative Prototype of Solar Chimney Power Plant, under Climatic Conditions in Ouagadougou, Burkina Faso. *Indian Journal of Science and Technology*. 2022;15(14):619–629. Available from: https://doi.org/10.17485/IJST/v15i14.1737.
7) Keshari SR, P CV, Das P. A 3D numerical study to evaluate optimum collector inclination angle of Manzanares solar updraft tower power plant. *Solar Energy*. 2021;226:455–467. Available from: https://doi.org/10.1016/j.solener.2021.08.062.
8) Das P, Chandramohan VP. 3D numerical study on estimating flow and performance parameters of solar updraft tower (SUT) plant: Impact of divergent angle of chimney, ambient temperature, solar flux and turbine efficiency. *Journal of Cleaner Production*. 2020;256:120353. Available from: https://doi.org/10.1016/j.jclepro.2020.120353.
9) Ganguli A, Deshpande S, Pandit A. CFD Simulations for Performance Enhancement of a Solar Chimney Power Plant (SCPP) and Techno-Economic Feasibility for a 5 MW SCPP in an Indian Context. *Energies*. 2021;14(11):3342. Available from: https://doi.org/10.3390/en14113342.
10) Semai H, Bouhdjar A. Effect of slope tower angle and thermal storage media on flexibility solar chimney power plant performance. *Environmental Progress & Sustainable Energy*. 2021;40(5):40. Available from: https://doi.org/10.1002/ep.13646.
11) Natarajan R, Jayaraman V, Sathyamurthy R. Comparative studies on performance of solar towers with variable scale ratios. *Environmental Science and Pollution Research*. 2022;29(30):45601–45611. Available from: https://doi.org/10.1007/s11356-022-19079-0.
12) Sundararaj M, Rajamurugu N, Anbarasi J, Yaknesh S, Sathyamurthy R. Parametric optimization of novel solar chimney power plant using response surface methodology. *Results in Engineering*. 2022;16:100633. Available from: https://doi.org/10.1016/j.rineng.2022.100633.
13) Semai H, Bouhdjar A. Impact of the chimney geometry on the power output of solar chimney power plant. *Thermophysics and Aeromechanics*. 2021;28(2):291–303. Available from: https://doi.org/10.1134/S0869864321020128.
14) Semai H, Bouhdjar A, Larbi S. Canopy slope effect on the performance of the solar chimney power plant. *International Journal of Green Energy*. 2017;14(3):229–238. Available from: https://doi.org/10.1080/15435075.2016.1253580.
15) Balijepalli R, Chandramohan VP, Kirankumar K, Suresh S. Numerical analysis on flow and performance characteristics of a small-scale solar updraft tower (SUT) with horizontal absorber plate and collector glass. *Journal of Thermal Analysis and Calorimetry*. 2020;141(6):2463–2474. Available from: https://doi.org/10.1007/s10973-020-10057-7.